

# Analysis of Ground Settlement of Double-Track Tunnel Undercrossing Shallow Overburden Silt Layer

Xingguo Yu<sup>1, 2, \*</sup>

<sup>1</sup>College of Geoscience and Engineering, North China University of Water Resources and Electric Power, Zhengzhou, 450046, China

<sup>2</sup>China Railway 16th Bureau Group Co., Ltd., Zhengzhou 450003, China

\* Corresponding author

**Abstract:** Taking the double-line shield tunnel of Zhengzhou Metro Line 12 undercrossing the shallow covered fine sand layer as the background, the construction process of the double-line shield tunnel undercrossing the shallow covered fine sand layer is simulated by using the measured data combined with the finite element analysis software. The surface settlement analysis under the conditions of single-line tunnel, double-line tunnel penetration and different tunnel spacing is focused, and the formula calculation data are compared with the numerical simulation results. The results show that the settlement curve calculated by Peck curve formula is similar to that of numerical simulation, and the correctness of the model is proved theoretically. During the process from the left tunnel through to the right tunnel through, the position of the maximum ground settlement value shifts from the center of the left tunnel to the center of the double-line tunnel, which is due to the influence of the secondary disturbance on the soil. The maximum ground settlement decreases with the increase of tunnel spacing, and the width of settlement trough increases with the increase of tunnel spacing.

**Keywords:** Tunnel; double lines; shallow cover; sedimentation.

## 1. Introduction

In recent years, with the rapid development of China's economy and the accelerated pace of urbanization, the number of permanent urban residents has continued to grow, leading to increasingly severe traffic congestion. To alleviate the pressure on urban transportation systems, the implementation of rail transit has become increasingly widespread<sup>[1]</sup>. The shield tunneling method has become the mainstream approach for constructing subway tunnels. As a highly efficient technique for tunnel excavation, it is adaptable to a wide range of geological conditions. However, the shield tunneling process can exert varying degrees of impact on the ground surface, potentially leading to serious safety incidents and irreversible economic losses. During the shield tunneling process, due to the confined nature of underground space and the complexity of geological conditions, it is common for the tunnel to pass beneath existing surface structures and underground facilities<sup>[2]</sup>. Therefore, in order to ensure the safety and stability of construction personnel as well as surface and underground structures, extensive attention has been paid by researchers and engineering professionals to the control and mitigation of ground settlement induced by shield tunneling<sup>[3][4][5]</sup>. Xu Xu<sup>[6]</sup> found that, upon the completion of excavation for both parallel tunnels, the maximum ground settlement occurred at the centerline between the two tunnels, and the magnitude of settlement gradually decreased toward both sides. Ralph B Peck<sup>[7]</sup> collected and analyzed a large volume of field-measured data from tunnel projects, and found that the ground settlement curve induced by tunnel excavation approximately follows a normal distribution. Based on this observation, he proposed the well-known Peck formula. Schmid<sup>[8]</sup> validated the Peck formula and further proposed that the width coefficient of the settlement trough in water-saturated plastic clay is influenced by both the tunnel radius and the depth of burial. Fang Enquan<sup>[9]</sup> building upon the Peck formula, proposed a predictive model that combines

interpolation and the least squares method, and utilized this model for ground settlement prediction. Yang Fengfeng<sup>[10]</sup> demonstrated that the Peck prediction curve needs to be modified in order to accurately predict the settlement of the soil above shield tunnels. Fu Chunqing<sup>[11]</sup> based on the Peck formula, introduced a section correction factor for in-depth modification studies. The modified Peck curve was found to align well with actual monitoring data, enabling more accurate predictions of construction-induced settlement using partial monitoring data. Liu Hongzhou<sup>[12]</sup> established a three-dimensional finite element model to analyze several factors influencing ground settlement during shield tunneling under soft soil conditions. Peng Chang<sup>[13]</sup> utilized the finite element software ABAQUS for three-dimensional numerical analysis to simulate ground settlement induced by shield tunneling. A comparison between the simulation results and field measurements demonstrated a high degree of agreement, thereby validating the reliability and practicality of the analytical method. Li Xiaoqing and Zhu Chuancheng<sup>[14]</sup> utilized finite element software to simulate the shield tunneling process and studied the effects of factors such as the internal friction angle, compression modulus, cohesion, Poisson's ratio, and tunnel burial depth on soil deformation. Overall, there is still relatively little research on ground settlement analysis in the case of dual-line shield tunnels passing through shallowly covered fine sand layers.

This study focuses on the shield tunneling section between Longzihu West Station and Longzihu Station on Zhengzhou Metro Line 12. Using finite element software for numerical simulation and integrating field measurement data, the ground settlement induced by shield tunneling beneath a shallowly covered fine sand layer is analyzed. The results provide valuable conclusions and offer relevant experience for similar future projects.

## 2. Theoretical Analysis of Ground Settlement Induced by Dual-Line Shield Tunneling

The ground settlement induced by shield tunneling in a single-tunnel excavation can be represented by the Peck formula. However, for a dual-tunnel excavation, the effects of ground settlement are additive and superimposed. Liu Bo<sup>[15]</sup> using the superposition principle, derived the formula for the lateral ground settlement of dual-tunnel excavations at the same burial depth:

$$S(x) = S_{\max 1} \exp\left[-\frac{(x+0.5L)^2}{2i_1^2}\right] + S_{\max 2} \exp\left[-\frac{(x-0.5L)^2}{2i_2^2}\right] \quad (0-1)$$

$$S_{\max 1} = \frac{V_{i1}}{i_1 \sqrt{2\pi}} \quad (0-2)$$

$$S_{\max 1} = \frac{V_{i2}}{i_2 \sqrt{2\pi}} \quad (0-3)$$

Where,  $S(x)$  represents the ground settlement at a horizontal distance  $x$  from the centerline of the dual-tunnel alignment;  $L$  is the center-to-center spacing between the two tunnels;  $S_{\max 1}$  and  $S_{\max 2}$  are the maximum settlements induced by the excavation of the first and second tunnels, respectively;  $V_{i1}$  and  $V_{i2}$  are the ground loss rates corresponding to the excavation of the first and second tunnels, respectively;  $i_1$  and  $i_2$  are the settlement trough width parameters resulting from the construction of the first and second tunnels, respectively. The transverse ground surface settlement profile for the dual-tunnel section is illustrated in Figure 1.

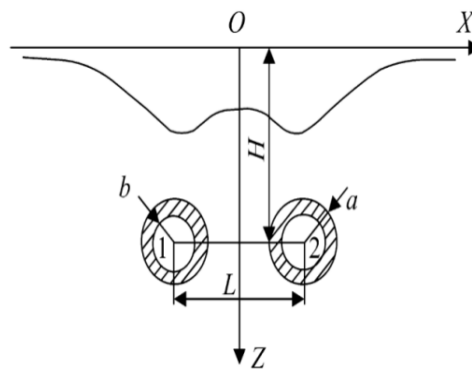


Figure 1. Schematic diagram of surface settlement of double-track tunnel cross-section

## 3. Project Overview

### 3.1. Project Background

The section from Longzihu West Station to Longzihu Station begins at Longzihu West Station and extends southeastward, passing beneath Longzihu Lake and aligning

along Ping'an Avenue before connecting to Longzihu Station. The tunnel section has a mileage range of DK20+129.55 to DK21+296.955 for the left line, with a total length of 1167.405 meters; and DK20+129.55 to DK21+297.816 for the right line, with a total length of 1168.266 meters, as shown in Figure 2.

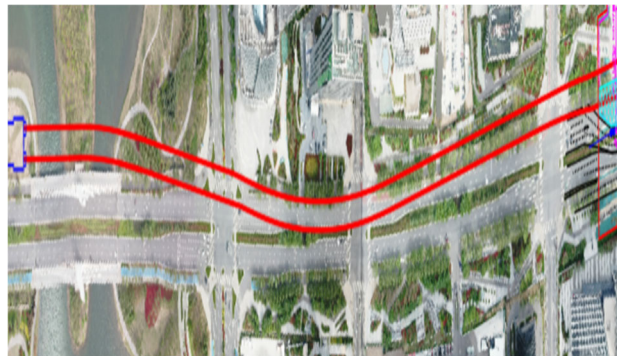


Figure 2. Schematic diagram of the alignment of the subway line

### 3.2. Engineering Geological Conditions

The section between Longzihu West Station and Longzihu Station mainly passes through silty clay, fine sand, and clayey silt layers. The engineering geological conditions in this area are relatively poor, characterized by medium to highly compressible soils with low strength and poor stability. The tunnel surrounding strata primarily consist of thick, water-

saturated sandy soils in a medium-dense to dense state. Groundwater is abundant, and the soil layers exhibit high permeability, making them prone to collapse, water ingress, and sand inflow during shield tunneling. Overall, the surrounding rock stability in this section is considered to be poor. The lithology of the strata along the section is shown in Table.

**Table 1.** Lithology of strata in the section of Zhengzhou Metro Line 12

Strata	Stratum Characteristics
Layer A②23: Silty Clay (Q4-2l)	Gray in color, ranging from hard plastic to plastic consistency, with medium dry strength, no reaction to shaking, slight gloss, and moderate toughness. Contains small amounts of organic matter and fragments of snail shells.
Layer A②33: Clayey Silt (Q4-1al+pl)	Yellow-brown to gray-brown in color, moist, medium-dense to dense, with low dry strength and low toughness. Exhibits a moderate reaction to shaking and no gloss. Contains small amounts of mica and iron oxides, with occasional fragments of snail shells. Locally interbedded with thin layers of silty clay and silt.
Layer A②52: Fine Sand (Q4-1al+pl)	Brown-yellow to brown-gray in color, saturated, medium-dense, with moderate particle gradation. The composition is primarily feldspar and quartz, containing iron oxides and mica flakes. In some local sections, the soil transitions to silty material.
Layer A②53: Fine Sand (Q4-1al+pl)	Brown-yellow to brown-gray in color, saturated, medium-dense to dense, with moderate particle gradation. The composition is mainly feldspar and quartz, containing iron oxides and mica flakes. In some local sections, the soil consists of silty material.
Layer A②54: Fine Sand (Q4-1al+pl)	Brown-yellow to brown-gray in color, saturated, medium-dense to dense, with generally moderate particle gradation. The composition is primarily feldspar and quartz, with the presence of iron oxides and mica flakes. In some local sections, the soil consists of silty material.
Layer A②55: Fine Sand (Q4-1al+pl)	Gray-brown to yellow-brown in color, saturated, dense, with generally moderate particle gradation. The composition is mainly feldspar and quartz, containing iron-manganese oxides and mica flakes, with occasional snail shell fragments.

## 4. Model Development and Numerical Analysis

tunneling section between Longzihu West Station and Longzihu Station on Metro Line 12, the physical parameters of the soil layers are summarized in Table 2.

### 4.1. Model Parameters

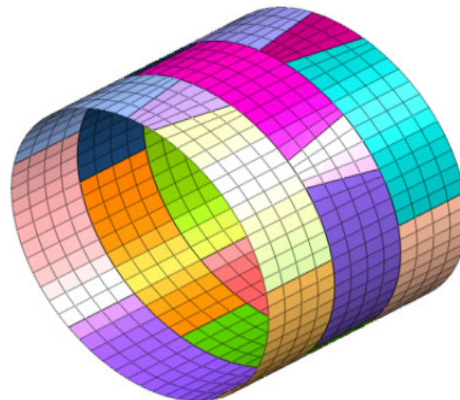
According to the geological survey report for the shield

**Table 2.** Physical parameters of each soil layer

Stratum Number	Stratum Name	Thickness (m)	Unit Weighty (KN/m <sup>3</sup> )	Compression Modulus (E/MPa)	Cohesion (C/kPa)	Friction Angle (°)	Poisson's Ratio
A①1	Artificial Fill	3.2	17.5	8	5	8.0	0.35
A②21	Silty Clay	4.3	18.3	4.2	21.5	11.5	0.37
A②52	Fine Sand 1	12.4	18.5	16.5	2	29	0.31
A②33	Clayey Silt	3.7	19	12.9	14	24	0.36
A②55	Fine Sand 2	26.4	19.5	28	1	33	0.30

The outer diameter of the shield tunnel lining is 6200 mm, the inner diameter is 5500 mm, the width is 1500 mm, and the thickness is 350 mm. The lining ring is assembled by three standard blocks of 67.5°, two adjacent blocks, and one wedge-

shaped block of 22.5°, arranged in a staggered pattern. The staggered assembly of the lining ring is shown in Figure 3. The physical parameters of the structural materials of the shield tunnel are provided in Table 3.

**Figure 3.** Diagram of misaligned joint assembly of lining rings

**Table 3.** Physical parameters of materials for various structures of shield tunnel

Structure	Density $\gamma$ (KN/m <sup>3</sup> )	Elastic Modulus (MPa)	Poisson's Ratio	Thickness (mm)	Concrete Grade
Segment	24.5	31050	0.17	350	C50
Grouting Material	24.5	30000	0.17	150	C30
Shield Shell	78.5	150000	0.35	50	—

### 4.2. Model Construction

(1) The finite element analysis model of a double-line shield tunnel beneath a shallow covering of fine sand, taking the Zhengzhou Metro Line 12 as the subject, is established. The simulation analysis of the excavation process is conducted. The dimensions of the soil model are 45m×50m×50m (length × width × height). The tunnel crown is located 12m beneath the ground surface, and the tunnel spacing is 13m. The grouting layer is modeled using solid elements, with shell elements extracted from the inner surface of the grouting layer to represent the shield tunnel segments, and from the outer surface to represent the shield shell. The grouting pressure is set to 200 kPa. The calculated face pressure is 300 kPa, and the jacking force is 12,000 kN. Normal constraints are applied to the soil around and beneath the tunnel, with the top being a free surface. A coupled relationship between the shield tunnel segments, grouting material, and soil is established. The structural model is shown in Figures 4 and 5.

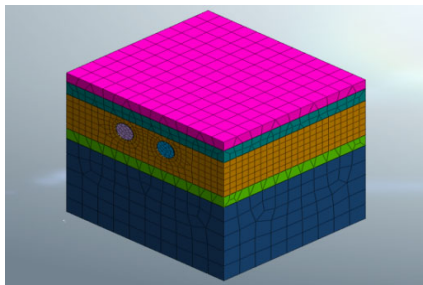


**Figure 4.** Diagram of soil structure model

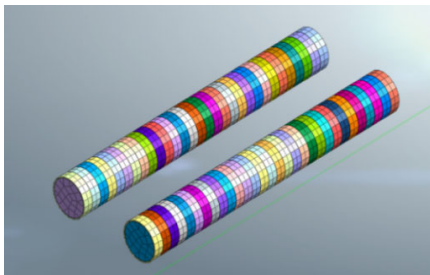


**Figure 5.** Diagram of tunnel structure model

#### (2) Model Assumptions

Due to the complexity of the geological conditions during shield tunneling, it is necessary to simplify the model appropriately to facilitate the calculations. The following are the assumptions made for the model:

- ① All soil layers in the model are assumed to be horizontally uniform in distribution.
- ② In the model, the excavated soil during shield tunneling and the grouting layer are both modeled using 3D solid elements. The shield shell and assembled lining segments are simulated using 2D shell elements. The segments, shield shell, and grouting layer are all considered as elastic materials.

- ③ The effects of groundwater are neglected.
- ④ The initial stresses consider only the self-weight of the soil layers and structures, as well as the automatic constraints.
- ⑤ In this model, after simulating the completion of shield tunneling, the consolidation settlement of the soil is not considered, meaning the time effect on the ground settlement process is neglected.
- ⑥ The model assumes a vertically aligned, straight parallel tunnel, neglecting the deflection curvature in the vertical and horizontal directions.

### 4.3. Settlement Calculation and Analysis

#### 4.3.1. The left-line tunnel is advanced first.

After the left-line tunnel is completed, as shown in Figure 6, the maximum ground settlement is 2.39 mm. The maximum settlement occurs directly above the left-line tunnel, and the ground settlement follows a normal distribution, decreasing symmetrically from the tunnel center to both sides. The maximum settlement of 3.32 mm occurs directly above the left tunnel, while the maximum heave of 5.48 mm is observed beneath the left tunnel. Using the centerline of the left tunnel as the axis, the maximum settlement,  $S_{max} = 2.4\text{mm}$ , is calculated. A comparison between the Peck formula settlement curve and the settlement curve obtained from numerical simulation is shown in Figure 7. It can be observed that the settlement curve obtained from the numerical simulation closely resembles the shape of the settlement curve calculated using the Peck formula.

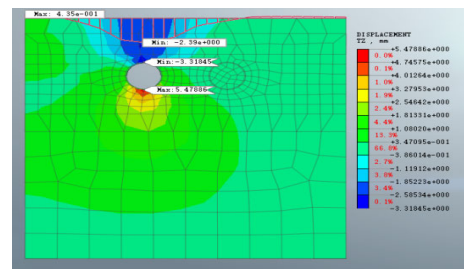


**Figure 6.** Surface Settlement Diagram during the Left-line Penetration

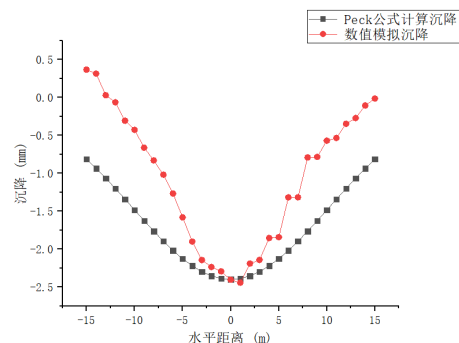


**Figure 7.** Comparison Diagram between Settlement Calculated by Peck Formula and Numerical Simulation

### 4.3.2. Double-Line Tunnel Completion

After both the left and right tunnels are fully completed, as shown in Figure 8, the maximum ground settlement is 2.33 mm. The position of the maximum settlement shifts from the centerline of the left tunnel towards the left of the centerline between the two tunnels. The settlement curve generally follows a normal distribution, with the settlement values decreasing from the center towards both sides. Meanwhile, the maximum settlement above the left tunnel increases to 2.94 mm, and the maximum heave beneath the left tunnel rises to 5.69 mm. Additionally, during the process from the completion of the left tunnel to the completion of the right tunnel, it can be observed that the position of the maximum ground settlement gradually shifts from the center of the left tunnel towards the center of the double-line tunnel.

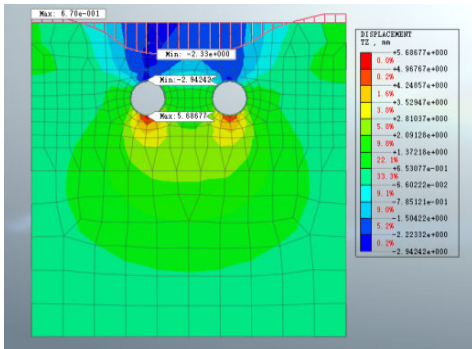
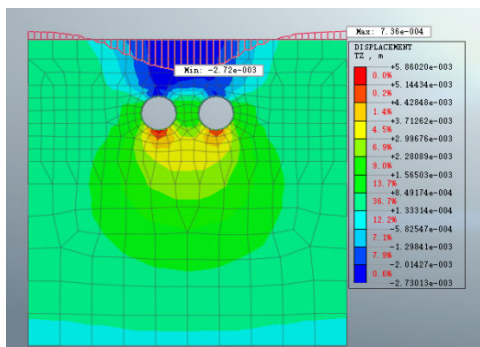


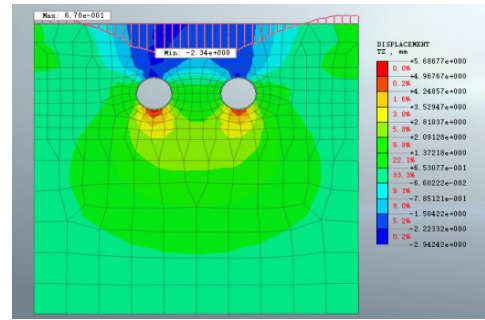
Figure 8. Surface Settlement Diagram during the Double-line Penetration

### 4.3.3. Analysis of the Impact of Tunnel Spacing on Ground Settlement in Shield Tunnels

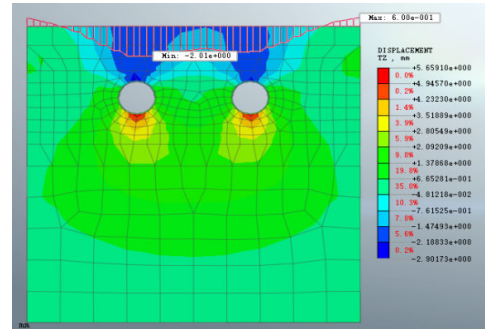
The tunnel spacing in the model was set to 9 m, 13 m, and 17 m, and numerical simulations were performed. As shown in Figure 9, when the tunnel spacing is 9 m, the ground settlement curve approximates a normal distribution with a maximum value of 2.72 mm. As the tunnel spacing increases to 13 m and 17 m, the ground settlement curve changes from a single-peak curve to a double-peak curve. The maximum settlement decreases as the tunnel spacing increases. The maximum settlement position is located at the bottom of the left tunnel's trough. This is because the left-line tunnel is excavated first, and when the right-line tunnel is excavated, it causes a secondary disturbance to the soil above the left-line tunnel, resulting in the maximum settlement being close to the left-line tunnel. Additionally, the width of the settlement trough increases as the tunnel spacing increases.



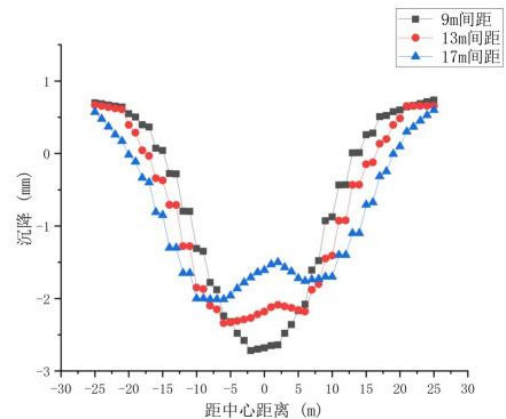
(a) Ground Settlement Contour Map for Tunnel Spacing of 9m



(b) Ground Settlement Contour Map for Tunnel Spacing of 13m



(c) Ground Settlement Contour Map for Tunnel Spacing of 17m



(d) Ground Lateral Settlement Profile for Full Line Completion at Different Tunnel Spacings

Figure 9. Surface Settlement Diagram of Double-track Tunnels with Different Spacings

## 5. Conclusion

- (1) The settlement curve obtained from the numerical simulation closely resembles the settlement curve calculated using the Peck formula, theoretically validating the correctness of the model.
- (2) The settlement curve generally follows a normal distribution, with the settlement values decreasing from the center towards both sides. When the double-line tunnel is completed, the position of the maximum ground settlement shifts from the center of the left tunnel towards the center of both the left and right tunnels.
- (3) As the tunnel spacing increases, the ground settlement curve changes from a single-peak curve to a double-peak curve. Additionally, the maximum ground settlement decreases with the increase in tunnel spacing, while the width of the settlement trough expands as the tunnel spacing increases.

## Acknowledgements

Research on the Evolution Mechanism of Geotechnical Deformation Disasters and Their Prevention and Judgment System, a Key Research and Development Special Project in Henan Province (241111321300) Technology for the Prevention and Control of Underground Traffic Disasters under Extreme Weather Conditions Based on Beidou and Remote Sensing Satellites (251111240800)

## References

- [1] Feng Zhentu, Shi Pengfei, Jiang Man, et al. Numerical Simulation Study on the Influence of Shield Machine Cutting Piles and Passing through a Composite Foundation on the Settlement of the Foundation of a Masonry House[J]. *Geotechnical Investigation & Surveying*, 2021, 49(09): 7-13.
- [2] Yan Hanbing. Construction of the Resilience Evaluation Index System for the Safety Management System of Shield Tunneling Construction[J]. *Construction & Design for Engineering*, 2025, (05): 257-259. DOI: 10.13616/j.cnki.gcjsysj.2025.03.080.
- [3] Li Jianqiang, Liang Xinyong, Zhu Jinxian. Study on Ground Surface Settlement Caused by Shield Tunnel Construction with Shallow Overburden[J]. *Engineering Construction*, 2023, 55(02): 29-35. DOI: 10.13402/j.gcjs.2023.02.019.
- [4] Wu Guanglei, Wen Liangtao. Analysis and Control of Settlement Deformation of Existing Buildings When Shield Construction Passes Beneath Them[J]. *Bulk Cement*, 2023, (05): 101-103 + 106.
- [5] Chen Hua. Research and Analysis on the Ground Surface Settlement Caused by Metro Shield Construction[J]. *Sichuan Cement*, 2018, (11): 255.
- [6] Xu Xu, Xue Yanyu, Zhang Zhenyu, et al. Study on the Influence Law of Settlement during the Construction of Double-line Shield Tunnels[J]. *Geotechnical Investigation & Surveying*, 2022, 50(04): 1-7 + 15.
- [7] Chen Chunlai, Zhao Chengli, Wei Gang, et al. Prediction of Soil Settlement Induced by Double-Line Shield Based on Peck Formula [J]. *Rock and Soil Mechanics*, 2014, 35(8): 2212-2218.
- [8] Song Kezhi, Wang Mengshu, Sun Mou. Reliability Analysis of Ground Surface Settlement of Shield Tunnel Based on Peck Formula [J]. *Journal of North Jiaotong University*, 2004(04): 30 - 33.
- [9] Fang Enquan, Yang Lingzhi, Li Pengfei. Research on Prediction of Ground Surface Settlement in Shield Construction Based on Modified Peck Formula [J]. *Modern Tunnelling Technology*, 2015, 52(1): 143 - 149.
- [10] Yang Fengfeng, Yan Hongbo, Tian Li, et al. Study on the Applicability of the Modified Peck Formula in Predicting the Ground Surface Settlement of Shield Tunnels in Water-rich Sand and Gravel Strata[J]. *Geotechnical Investigation & Surveying*, 2021, 49(11): 72-78.
- [11] Fu Chunqing, Tian Shiwen, Liu Bo, et al. Application of the Modified Peck Formula in the Settlement Prediction of Sand and Gravel Strata in Beijing Area[J]. *Construction Technology*, 2020, 49(09): 74-77.
- [12] Liu Hongzhou, Sun Jun. Numerical Study on Influencing Factors of Ground Settlement in Shield Driving of Soft Soil Tunnel [J]. *Modern Tunnelling Technology*, 2001(6): 24 - 28.
- [13] Peng Chang, Ji Yulin, Luo Hanbin, et al. Numerical Analysis of the Influence of Double-line Shield Construction on Adjacent Buildings[J]. *Chinese Journal of Rock Mechanics and Engineering*, 2008(S2): 3868 - 3874.
- [14] Li Xiaoqing, Zhu Chuncheng. Numerical Analysis and Research on Ground Surface Settlement in Shield Tunnel Construction [J]. *Journal of Highway and Transportation Research and Development*, 2007(06): 86 - 91.
- [15] Liu Bo, Tao Longguang, Ding Chenggang, et al. Prediction Research and Application of Ground Surface Settlement Induced by Metro Double-tunnel Construction[J]. *Journal of China University of Mining & Technology*, 2006, (03): 356-361.